^{195}Pt NMR Kinetic and Mechanistic Studies of *cis*- and *trans*-Diamminedichloroplatinum(II) Binding to DNA

Daniel P. Bancroft, Christopher A. Lepre, and Stephen J. Lippard*

Contribution from the Department of Chemistry, Massachusetts Institute of Technology, Cambridge, Massachusetts 02139. *Received March 9, 1990*

Abstract: The kinetics and mechanism of binding of the anticancer drug *cis*-diamminedichloroplatinum(II), or *cis*-DDP, and its inactive trans isomer to chicken erythrocyte DNA at 37 °C have been investigated by ^{195}Pt NMR spectroscopy. Both *cis*- and *trans*-DDP bind to DNA by two successive pseudo-first-order processes, forming monofunctional adducts (^{195}Pt NMR shifts near −2300 ppm) that subsequently close to bifunctional lesions (chemical shifts near −2450 ppm). The pseudo-first-order rate constants at pH 6.5 and 37 °C for the first DNA binding step are $k = 10.2 \pm 0.7 \times 10^{-5}$ s^{-1} ($t_{1/2} = 1.9 \pm 0.1$ h) for *cis*-DDP and $k = 9.6 \times 10^{-5}$ s^{-1} ($t_{1/2} = 2.0 \pm 0.1$ h) for *trans*-DDP. These rate constants are the same as for the rate of hydrolysis of the first chloride ion in this solution. The monofunctional adducts are bound predominantly at the N7 position of guanosine and retain a chloride ligand. The pseudo-first-order rate constants at pH 6.5 and 37 °C for closure of mono- to bifunctional adducts are $9.2 \pm 1.4 \times 10^{-5}$ s^{-1} ($t_{1/2} = 2.1 \pm 0.3$ h) and $6.3 \pm 0.1 \times 10^{-5}$ s^{-1} ($t_{1/2} = 3.1 \pm 0.1$ h) for the cis and trans isomers, respectively, and are the same for closure on single-stranded DNA. These results indicate that the different biological activities of *cis*- and *trans*-DDP cannot, as others have suggested, be due to large differences in monofunctional adduct lifetimes. The similarity of the rate constants for monofunctional adduct closure to those for the second hydrolysis of *cis*-DDP and the absence of significant concentrations of aquated species in the reaction mixture indicate that loss of chloride is the rate-limiting step in monofunctional adduct closure. The $\Delta S^{\ddagger}$ and $\Delta H^{\ddagger}$ values for monofunctional adduct closure are comparable to those for substitution reactions of square-planar Pt(II) complexes. The closure reactions are proposed to proceed through solvent-associated intermediates. Both *cis*- and *trans*-DDP monofunctional, but not bifunctional, adducts react rapidly with glutathione, forming sulfur-bound species with ^{195}Pt NMR chemical shifts near −2900 ppm that are trapped and cannot close to form bifunctional lesions. Preliminary experiments indicate that *trans*-DDP monofunctional adducts react more rapidly with glutathione than those of the cis isomer, suggesting that selective trapping of *trans*-DDP monofunctional adducts in vivo could contribute to the biological inactivity of this isomer.

It is widely accepted that the anticancer drug cisplatin, *cis*-diamminedichloroplatinum(II) or *cis*-DDP,[1] manifests its therapeutic activity by binding directly to DNA, deactivating it as a template for replication and possibly transcription as well.[2] A long-standing question has been why the trans isomer, which differs

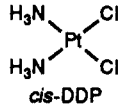

cis-DDP

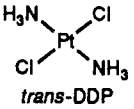

trans-DDP

only in its ligand coordination geometry, is less mutagenic, less cytotoxic, and ineffective as an antitumor agent. Although a much larger dose of *trans*-DDP than *cis*-DDP is required to bind an equal number of platinum atoms per nucleotide, bifunctional adducts of the two isomers inhibit replication to the same extent.[3-5] It has been proposed that selective removal of bound *trans*-DDP from DNA may account for the difference in activities.[4]

The binding of *cis*- and *trans*-DDP to DNA is kinetically, rather than thermodynamically, controlled. The rate-limiting step for initial binding is hydrolysis of the first chloride ion,[6-8] after which the complexes coordinate primarily to the N7 positions of guanine and adenine bases, which are accessible in the major groove, to form monofunctional adducts. These monofunctional adducts subsequently react with a second nucleophile, forming primarily intrastrand adducts in vitro, at d(GpG) and d(ApG) sequences for the cis,[9-15] and at d(GpNpG) and d(CpNpG) (N is any base) sequences for the trans, isomer.[16-19] Differences between the activities of the two isomers may arise from differences in the lifetimes or reactivities of their monofunctional DNA adducts. In particular, Butour and Johnson reported half-lives for closure of monofunctional to bifunctional adducts to be 15 and 30 h for the cis and trans isomers, respectively.[20] Eastman and Barry[16] observed closure of *trans*-DDP monofunctional adducts to be only half complete within 24 h on double-stranded DNA, but at least twice as fast on single-stranded DNA. In contrast, there are numerous reports[11,15,18,22,23] of much shorter lifetimes for the

(1) Abbreviations: *cis*-DDP, *cis*-diamminedichloroplatinum(II); *trans*-DDP, *trans*-diamminedichloroplatinum(II); $(D/N)_f$, formal drug-to-nucleotide ratio; $(D/N)_b$, bound drug-to-nucleotide ratio; NMR, nuclear magnetic resonance; HPLC, high-performance liquid chromatography; *cis*-MFA, *cis*-{Pt$(NH_3)_2$Cl}$^+$-DNA monofunctional adduct(s); *trans*-MFA, *trans*-{Pt$(NH_3)_2$Cl}$^+$-DNA monofunctional adduct(s); *cis*-BFA, *cis*-{Pt$(NH_3)_2$}$^{2+}$-DNA bifunctional adduct(s); *trans*-BFA, *trans*-{Pt$(NH_3)_2$}$^{2+}$-DNA bifunctional adduct(s).

(2) For recent reviews, see: (a) Sherman, S. E.; Lippard, S. J. *Chem. Rev.* **1987**, *87*, 1153. (b) Reedijk, J. *Pure Appl. Chem.* **1987**, *59*, 181. (c) Eastman, A. *Pharmac. Ther.* **1987**, *34*, 155. (d) Roberts, J. J. *Pontificiae Academiae Scientarium Scripta Varia* **1988**, *70*, 464. (e) Pinto, A. L.; Lippard, S. J. *Biochim. Biophys. Acta* **1985**, *780*, 167.

(3) Salles, B.; Butour, J.-L.; Lesca, C.; Macquet, J.-P. *Biochem. Biophys. Res. Commun.* **1983**, *112*, 555.

(4) Ciccarelli, R. B.; Solomon, M. J.; Varshavsky, A.; Lippard, S. J. *Biochemistry* **1985**, *24*, 7533.

(5) Heiger-Bernays, W.; Essigmann, J. M.; Lippard, S. J. *Biochemistry*. In press.

(6) Johnson, N. P.; Hoeschele, J. D.; Rahn, R. O. *Chem.-Biol. Interactions* **1980**, *30*, 151.

(7) Ushay, H. M.; Tullius, T. D.; Lippard, S. J. *Biochemistry* **1981**, *20*, 3744.

(8) Bodenner, D. L.; Dedon, P. C.; Keng, P. C.; Borch, R. F. *Cancer Res.* **1986**, *46*, 2745.

(9) Eastman, A. *Biochemistry* **1983**, *22*, 3927.

(10) Eastman, A. *Biochemistry* **1985**, *24*, 5027.

(11) Eastman, A. *Biochemistry* **1986**, *25*, 3912.

(12) Eastman, A. *Chem.-Biol. Interactions* **1987**, *61*, 241.

(13) Johnson, N. P.; Mazard, A. M.; Escalier, J.; Macquet, J. P. *J. Am. Chem. Soc.* **1985**, *107*, 6376.

(14) Fichtinger-Schepman, A. M.; Lohman, P. H.; Reedijk, J. *Nucl. Acids Res.* **1982**, *10*, 5345.

(15) Fichtinger-Schepman, A. M.; van der Veer, J. L.; Lohman, P. H.; Reedijk, J. *Biochemistry* **1985**, *24*, 707.

(16) Eastman, A.; Barry, M. A. *Biochemistry* **1987**, *26*, 3303.

(17) Eastman, A.; Jennerwein, M. M.; Nagel, D. L. *Chem.-Biol. Interactions* **1988**, *67*, 71.

(18) Fichtinger-Schepman, A. M.; Dijt, F. J.; De Jong, W. H.; van Oosterom, A. T.; Berends, S. F. In *Platinum and other metal coordination complexes in cancer chemotherapy*; Nicolini, M., Ed.; Nijhof: Boston, 1988, p 33.

(19) Royer-Pokora, B.; Gordon, L. K.; Haseltine, W. A. *Nucl. Acids Res.* **1981**, *9*, 4595.

(20) Butour, J.-L.; Johnson, N. P. *Biochemistry* **1986**, *25*, 4534.

(21) Pinto, A. L.; Lippard, S. J. *Proc. Natl. Acad. Sci. U.S.A.* **1985**, *82*, 4616.

(22) Schaller, W.; Reisner, H.; Holler, E. *Biochemistry* **1987**, *26*, 943.

0002-7863/90/1512-6860$02.50/0

cis-DDP monofunctional adducts. For example, Malinge and Leng found such adducts to disappear with a pseudo-first-order rate constant k of 4.5–5 × 10^{-5} s^{-1}, corresponding to a half-life of ~4 h.[23]

These different kinetic results may derive from the use of various chemical agents, including thiourea, ammonium bicarbonate, guanosine, and ethidium bromide, to trap platinum adducts in their monofunctional state. Such an approach is indirect and inherently invasive. Its success requires not only that the agent be reactive enough to trap monofunctional adducts before they can close, to preclude measuring erroneously low levels of monofunctional adducts, but also that it not remove such adducts from DNA. In addition, the trapping agent must react rapidly with any unbound *cis*- or *trans*-DDP in solution to form complexes that are incapable of binding to DNA; otherwise, anomalously high levels of monofunctional adducts will be scored. Moreover, if results for *cis*- and *trans*-DDP are to be compared, the trapping reagent must react with monofunctional adducts of both isomers at comparably rapid rates. A further shortcoming of the chemical trapping approach is its inability to discern whether Cl^-, H_2O, OH^-, or some other ligand remains in the platinum coordination sphere of the monofunctional adduct, since this ligand is replaced by the trapping agent.

The principal objective of the work reported here has been to determine the kinetics and mechanism of *cis*- and *trans*-DDP binding to DNA, with particular emphasis on determining the lifetimes of monofunctional adducts, using the noninvasive technique of ^{195}Pt NMR spectroscopy. This approach makes it possible to identify and follow the evolution of species formed during platination reactions and to elucidate the rate-determining steps in the formation and closure of the monofunctional adducts.

An additional objective has been to investigate the effect of glutathione upon the closure of *cis*- and *trans*-DDP monofunctional adducts. Sulfur-containing nucleophiles such as glutathione, typically found at 2–5 mM concentrations in cells,[24] and serum albumin (0.7 mM)[25] can interfere with *cis*- and *trans*-DDP binding to DNA in vivo by two mechanisms. First, they may directly coordinate platinum in plasma or cytosol;[25-28] *trans*-DDP reacts with glutathione 300 times more rapidly than *cis*-DDP, possibly accounting for the difference in dose required to afford equal amounts of bound platinum per nucleotide.[26,29] Second, glutathione and other intracellular nucleophiles can bind at the labile site of monofunctional adducts and prevent them from closing.[8,12,16,29] In this process, the relative lifetimes of the *cis*- and *trans*-DDP monofunctional adducts, their relative affinities toward glutathione, and the effects of trans-labilization due to S-bound glutathione all become potentially important. Moreover, glutathione reacts in vitro with *cis*-DDP monofunctional adducts without saturating them,[12] whereas reaction with *trans*-DDP monofunctional adducts proceeds rapidly to saturation.[16] Since the rate of platinum removal by glutathione is slow compared to cellular repair processes, only 30% of the *trans*-DDP monofunctional adducts being lost over 20 h, it was postulated that differences in activity between the two isomers may be the result of selective trapping of trans monofunctional adducts by glutathione.[16] The present ^{195}Pt NMR studies provide new insights into the fundamental inorganic chemistry underlying these phenomena.

Experimental Section

Preparation of Chicken Erythrocyte DNA. Chicken erythrocyte DNA was isolated from whole blood and purified by using a protocol adapted from published procedures.[30-33] Specifically, DNA obtained from trimmed nucleosome cores was digested into double-stranded fragments of between 20 and 60 bp in length by using DNase II and S1 nuclease in a modification of the procedure of Early and Kearns.[33] This step increases its solubility, facilitating NMR spectroscopic study. Aliquots containing 60 mg each of DNA were measured out and lyophilized to dryness prior to storage at −20 °C. The sizing of DNA fragments was checked by gel electrophoresis on a non-denaturing 17% polyacrylamide gel, which revealed ~40 bp average lengths.

Synthesis of ^{195}Pt-Enriched Platinum Compounds. Isotopically enriched (97.28% ^{195}Pt, Oak Ridge National Laboratories) K_2PtCl_6, *cis*-DDP, and *trans*-DDP were synthesized from platinum metal with use of literature methods.[34] $[^{195}Pt]Na_2[PtCl_6]$ was prepared for use as a ^{195}Pt NMR chemical shift standard from $[^{195}Pt]K_2[PtCl_6]$ by cation exchange over Bio-Rex 70 resin (Bio-Rad).

Preparation of Samples for Kinetic Studies of DNA Binding. Reactions were initiated by addition of predissolved $[^{195}Pt]$*cis*-$[Pt(NH_3)_2Cl_2]$, *trans*-$[Pt(NH_3)_2Cl_2]$, or solutions of the monoaquated analogues, prepared as described below, dissolved in 3 mM sodium chloride, 1 mM sodium phosphate, pH 6.5 or 7.4, to lyophilized chicken erythrocyte DNA. Immediately after addition of the platinum complexes, the reaction mixtures were transferred to an NMR tube and inserted into the NMR spectrometer. Single-stranded DNA was obtained by heating predissolved samples of double-stranded DNA in boiling water for 5 to 10 min followed by rapid cooling on ice prior to addition of the platinum complexes. Kinetics experiments performed at pH 6.5 or 7.4 revealed no differences in the rates of closure for either *cis*- or *trans*-DDP monofunctional adducts. As expected from the stoichiometry of the reactions, the pH did not change significantly over the course of the NMR experiments. In the case of samples containing glutathione, the pH was observed to drop by varying degrees during the course of the reaction, depending upon the amount of added glutathione.

Reactions of *cis*- and *trans*-DDP with DNA. In a typical experiment, *cis*-DDP (3.8 mg, 13 μmol) was dissolved in 800 μL of aqueous solution by rapidly heating the mixture to near boiling and vigorously vortexing the resulting solution. Subsequent centrifugation revealed the absence of any undissolved material. The cooled solution was then added to 60 mg of lyophilized chicken erythrocyte DNA prepared as described above. In no case was precipitation of *cis*-DDP observed upon addition to the DNA. The small amount of hydrolyzed *cis*-DDP initially introduced into the samples by use of this procedure has no effect upon the subsequent kinetic analysis, in which loss of unhydrolyzed cisplatin with time is monitored under pseudo-first-order conditions. Final concentrations of platinum and DNA as measured by atomic absorption and UV spectroscopy varied somewhat from the target values of 16 and 227 mM, respectively, owing to variations incurred in the preparation of the samples. The drug-to-nucleotide ratios ($(D/N)_b$'s) were typically within 15% of the desired values. Independent studies of the platinum concentrations of saturated solutions of *cis*-DDP prepared by dissolution in the absence of DNA for 1–24 h at 37 °C were measured to be 11.1–15.6 mM by atomic absorption spectroscopy. An experiment was carried out further to demonstrate that heating the *cis*-DDP solutions did not significantly affect the kinetics of the initial DNA binding reaction. A saturated *cis*-DDP solution was prepared by vigorously shaking 3.8 mg of *cis*-DDP in 50 μL of DMF and 35 μL of aqueous solution at 37 °C for 15 min. The solution was quickly centrifuged and the supernatant added to ~110 mg of DNA that had been previously dissolved in 715 μL of aqueous solution. The rate constant for this reaction (Table III, entry 2) was the same as that obtained for reactions using samples in which the solutions were heated above 37 °C to assist dissolution of the *cis*-DDP.

The *trans*-DDP reactions were performed by using saturated 800-μL aqueous solutions prepared with heating and centrifugation as described above for *cis*-DDP. Undissolved *trans*-DDP was removed by centrifugation prior to introduction of the solutions to the lyophilized DNA. As in the case of the *cis*-DDP reactions, no precipitation occurred upon addition to the DNA.

Reactions of *cis*- and *trans*-$[Pt(NH_3)_2(H_2O)Cl]^+$ with DNA. $[^{195}Pt]$*cis*-$[Pt(NH_3)_2(H_2O)Cl]^+$ was generated by allowing *cis*-DDP (7.6 mg, 25.3 μmol) to react with 1.2 equiv of $AgNO_3$ in 50 μL of di-

(23) Malinge, J.-M.; Leng, M. *Nucl. Acids Res.* **1988**, *16*, 7663.
(24) Kosower, N. S.; Kosower, E. M. *Int. Rev. Cytol.* **1978**, *54*, 109.
(25) Momburg, R.; Bourdeaux, M.; Sarrazin, M.; Chauvet, M.; Briand, C. *J. Pharm. Pharmacol.* **1987**, *39*, 691.
(26) Dedon, P. C.; Borch, R. F. *Biochem. Pharmacol.* **1987**, *36*, 1955.
(27) Norman, R. E.; Sadler, P. J. *Inorg. Chem.* **1988**, *27*, 3583.
(28) Odenheimer, B.; Wolf, W. *Inorg. Chim. Acta* **1982**, *66*, L41.
(29) Borch, R. F.; Dedon, P. C.; Gringeri, A.; Montine, T. J. In *Platinum and other metal coordination complexes in cancer chemotherapy*; Nicolini, M., Ed.; Nijhof: Boston, 1988; p 216.
(30) Granot, J.; Feigon, J.; Kearns, D. R. *Biopolymers* **1982**, *21*, 181.
(31) Tatchell, K.; van Holde, K. E. *Biochemistry* **1977**, *16*, 5295.
(32) Shaw, B. R.; Herman, T. M.; Kovacic, R. T.; Beaudreau, G. S.; van Holde, K. E. *Proc. Natl. Acad. Sci. U.S.A.* **1976**, *73*, 505.
(33) Early, T.; Kearns, D. R. *Proc. Natl. Acad. Sci. U.S.A.* **1979**, *76*, 4165.
(34) (a) Grube, H. L. In *Handbook of Preparative Inorganic Chemistry*; 2nd ed.; Brauer, G., Ed.; Academic Press Inc.: New York, 1965; Vol. II, pp 1560–1573. (b) Keller, R. N. In *Inorganic Syntheses*; McGraw-Hill Book Co. Inc.: New York, 1963; Vol. 7, pp 232–245. (c) Kauffman, G. B.; Teter, L. A.; Cowan, D. O. In *Inorganic Syntheses*; McGraw-Hill Book Co. Inc.: New York, 1946; Vol. 2, pp 247–253. (d) Dhara, S. C. *Ind. J. Chem.* **1970**, *8*, 193.

methylformamide for 16–24 h at 37 °C in the dark with vigorous shaking. The AgCl precipitate was subsequently removed by centrifugation, and the yellow supernatant containing [^{195}Pt]*cis*-[$Pt(NH_3)_2(DMF)Cl]^+$ was added to 750 μL of 1 mM Na_2HPO_4, 3 mM NaCl, pH 6.5, containing 120 mg of freshly dissolved chicken erythrocyte DNA. The weakly coordinated DMF ligand is replaced by water upon addition of the supernatant to the aqueous DNA solution. The final solution contained ~6.3% DMF, which does not interfere with subsequent Pt-DNA binding. A similar procedure was used to generate [^{195}Pt]*trans*-[$Pt(NH_3)_2(H_2O)Cl]^+$. The reaction with $AgNO_3$ was more efficient with the trans isomer, so that only 1 equiv of $AgNO_3$ was required and the reaction was complete within 2 h. The final reaction mixtures for these studies were formally 32 mM in Pt and 455 mM in DNA nucleotides, giving a drug-to-nucleotide ratio, $(D/N)_f$, of 0.07. As described above for the *cis*-DDP reactions, the concentration values varied somewhat from sample-to-sample; however, since pseudo-first-order conditions were maintained, these variances had no effect on the kinetic analyses of the data. For reactions run in the presence of glutathione, DNA was allowed to incubate with [^{195}Pt]*cis*- and *trans*-[$Pt(NH_3)_2(H_2O)Cl]^+$ for 20 min at 37 °C in order to consume free platinum species by forming monofunctional adducts, after which time small aliquots of freshly prepared 1.0 M solutions of reduced glutathione were added to give the desired final concentration.

UV and Atomic Absorption Spectroscopy. A Perkin-Elmer Lambda 7 spectrophotometer was used to measure DNA concentrations. Platinum was determined with a Varian 1475 Series atomic absorption spectrophotometer equipped with a GTA-95 graphite furnace. During the course of measuring the platinum concentrations, we observed an isotope effect arising from use of the ^{195}Pt-enriched samples. In particular, absorbance values were only 55% of those expected, since the platinum emission band from the natural abundance source of the hollow cathode lamp in the spectrometer is slightly shifted relative to the ^{195}Pt-absorption line. Anomalously low $(D/N)_b$ values are measured as a consequence of this shift. Although such isotope effects have apparently not been previously encountered in platinum atomic absorption spectroscopy, they have been reported for other elements.[35] Final platinum concentrations for samples enriched with ^{195}Pt were obtained by dividing the apparent concentrations by 0.55. This value was obtained by comparing results for both enriched and natural abundance samples of K_2PtCl_4 and *cis*-DDP.

^{195}Pt NMR Spectroscopy. ^{195}Pt NMR spectra were obtained by using a Varian VXR-500 NMR spectrometer operating at 107.3 MHz, equipped with a 5-mm tunable broadband probe and a VXR-5000 data system (VNMR software version 2.1, Sun Microsystems 3/60 computer). The temperature was regulated with an Oxford VTC4 controller that was calibrated to within ±0.3 °C by using ethylene glycol. Individual transients of 1024 complex data points each were accumulated over a 100-KHz spectral window with use of an acquisition time of 5 ms (collection rate of 200000 transients per hour), a 16-μs (90°) pulse, and a filter bandwidth of 49.5 KHz. The delay between the acquisition pulse and the onset of data collection was 10 μs. No decoupling was used. The spectrometer was frequency locked on deuterium and shimmed by using a standard sample of 0.1 M K_2PtCl_4 in 0.1 M DCl. Spectra for kinetics analyses were acquired without frequency locking and referenced to external K_2PtCl_4 standard (−1623 ppm relative to [^{195}Pt]Na_2PtCl_6 in water at 37 °C). The free induction decays were summed, zero filled to 8096 points, weighted with a 200-Hz exponential line-broadening factor, and processed with standard Fourier transform techniques. The spectra were baseline corrected prior to integration by third-order polynomial fitting to predefined baseline regions. A typical DNA kinetics experiment run at 37 °C consisted of a set of spectra, each comprised of 100000 or 200000 transients (30 or 60 min collection time), acquired over a period of 14–16 h (a minimum of 3 half-lives). Collection times of 30 min and 100000 transients were used for the experiments run at 45 °C.

The magnitude of the magnetic field drift during the course of a typical unlocked 16-h experiment was measured by comparing the frequency of the external reference line before and after the kinetics run. The magnetic field drifted by less than 20 Hz out of 103.7 MHz, which results in an imperceptible error in the integrated peak areas. The variation in the measured peak areas arising from baseline noise and random or systematic changes in the transmitter and receiver systems was measured by performing several runs with an internal standard of (PPh_4)-$[Pt(NH_3)Cl_3]$ in DMF sealed in a 1-mm capillary. The magnitude of scatter in peak areas was measured from the integral of the internal standard resonance. During the course of a typical 16-h kinetics experiment, the area of the internal standard resonance had a relative standard deviation of 7.6% or less. The standard resonance had an area that was seven times less than that of the *cis*-DDP resonance, and thus the relative standard deviation of the standard peak area serves as a measure of upper limit of the standard deviation for the *cis*-DDP resonance for reaction times up to approximately 3 half-lives. There was no apparent systematic drift in the standard peak area. In order to eliminate any changes in peak intensities arising from fluctuations in the acquisition hardware, which would affect all resonances equally, the reactant peak areas were normalized by dividing them by the area of the internal standard peak. The rate constants calculated by using this method were within ±10% of those calculated from the absolute areas, but they were less precise owing to the propagation of error from two integral measurements.

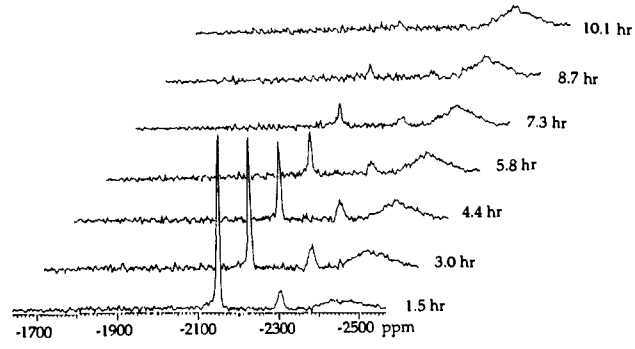

Figure 1. Time-dependent ^{195}Pt NMR spectra of the reaction between *cis*-DDP and chicken erythrocyte DNA at 37 °C in 3 mM NaCl, 1 mM NaH_2PO_4, at a drug-to-nucleotide ratio (D/N) of 0.07.

Analysis of Kinetics Data. Pseudo-first-order rate constants (k) were obtained from the slopes of linear least-squares fits to plots of ln (peak area) vs the reaction time, by using data collected over at least 3 half-lives.[36] The last few data points were sometimes omitted from the kinetic analyses because random spectral noise prevented accurate integration of low intensity peaks. In some experiments, successive spectra were added together (1 + 2, 2 + 3, etc.) in order to improve the signal-to-noise ratio. Kinetics parameters calculated from these sum spectra were within 3% of values obtained by using individual spectra. Unless stated otherwise, all rate constants quoted refer to pH 6.5.

Whenever possible, the experimentally determined values for the rate parameters k and $t_{1/2}$ are reported with the standard deviation from replicate experiments. In the Eyring plots, the error bars in the ln (k/T) dimension represent the standard deviation (4 to 14%) in k from the slope of the linear least-squares fit used to calculate k at the given temperature, except for data measured at 37 °C, for which the standard deviation of replicate experiments (15%) was used. The error in rate constants arising from the uncertainty in the reaction temperature was calculated to be 3.3%. The uncertainties in the activation parameters were calculated from the standard deviation of the slope and intercept of the linear least-squares fit to the plot of ln (k/T) vs $1/T$.

Results and Discussion

Reaction of *cis*-DDP with Double-Stranded DNA. The time course of the reaction between *cis*-DDP and double-stranded DNA is shown in Figure 1. *cis*-DDP (^{195}Pt resonance, −2149 ppm) is consumed with concomitant appearance of monofunctional intermediates (near −2300 ppm) which were then converted to bifunctional adducts (near −2500 ppm). There are no other platinum-containing species observed in the region from −1300 to −3400 ppm. As discussed later, these chemical shifts correspond to the sequential replacement of chloride by nucleobase N-donors in the platinum coordination sphere.

As reported by other workers,[6-8,37,38] the first step of *cis*-DDP binding to DNA is controlled by the rate of hydrolysis. The consumption of *cis*-DDP in the presence of a 14-fold excess of DNA bases ($(D/N)_f$ 0.07) is pseudo-first-order, as revealed by the linear plot of ln [*cis*-DDP] vs reaction time in Figure 2. The pseudo-first-order rate constant for the disappearance of *cis*-DDP in the presence of DNA is $10.2 \pm 0.7 \times 10^{-5}$ s^{-1} ($t_{1/2} = 1.9 \pm 0.1$

(35) Reynolds, R. J.; Aldous, K.; Thompson, K. C. In *Atomic Absorption Spectroscopy: A Practical Guide*; Barnes & Noble, Inc.: New York, 1970; pp 184–190.

(36) Espenson, J. H. *Chemical Kinetics and Reaction Mechanisms*; McGraw-Hill: New York, 1981; and references therein.

(37) Macquet, J.-P.; Theophanides, T. *Bioinorg. Chem.* **1975**, *5*, 59.

(38) Segal, E.; Le Pecq, J.-B. *Cancer Res.* **1985**, *45*, 492.

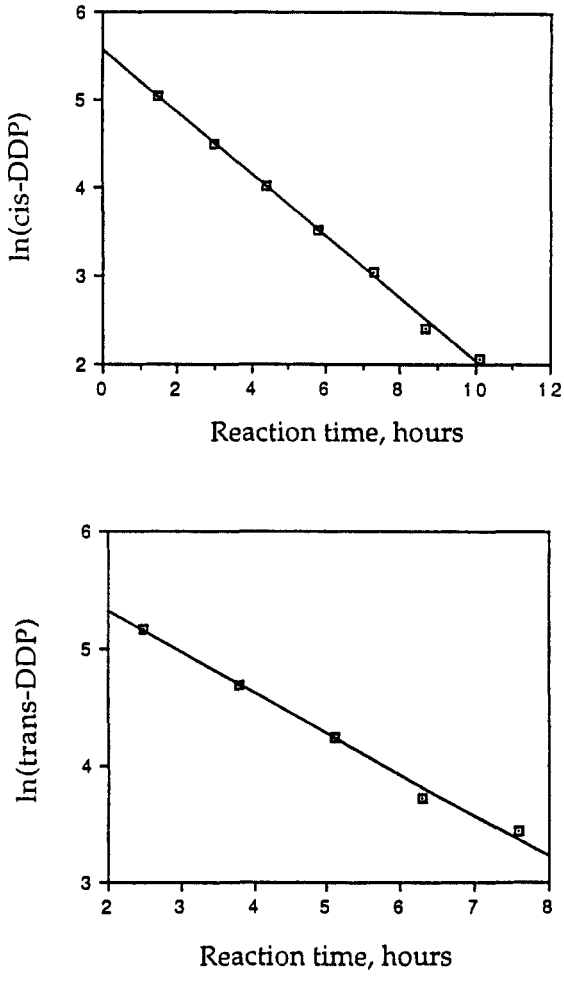

Figure 2. Determination of the rate constant for the reactions of *cis*- and *trans*-DDP with DNA. Top: plot of ln (*cis*-DDP) vs reaction time, where (*cis*-DDP) is the integrated area of the *cis*-DDP resonances from the data in Figure 1. Bottom: plot of ln (*trans*-DDP) vs reaction time, where (*trans*-DDP) is the integrated area of the *trans*-DDP resonances (data not shown).

h, average of ten experiments) at 37 °C and pH 6.5. When the reaction was carried out at a significantly lower $(D/N)_b$ (0.02) and higher pH (7.5), the same rate constant was obtained, $k = 9.3 \times 10^{-5}$ s^{-1}. The invariance of the rate constant with *cis*-DDP concentration is further proof of pseudo-first-order behavior. The same rate constant, $k = 10.9 \pm 0.1 \times 10^{-5}$ s^{-1} (two experiments), was also observed when the reaction was carried out with single-stranded DNA.

In order to demonstrate that the rate of the initial binding of *cis*-DDP to DNA is the same as the rate of hydrolysis under our conditions, we measured the hydrolysis of *cis*-DDP in our solutions at 37 °C. The rate constant for this reaction was difficult to determine precisely because, in the absence of a nucleophile to coordinate the aquated species and prevent its back-reaction with chloride, the reaction reaches equilibrium within 1 h. A similar problem was noted by Martin.[39] By using short (6 min) NMR collection times, it was possible to measure a first-order rate constant of $9.5 \pm 1.3 \times 10^{-5}$ s^{-1} for the hydrolysis of *cis*-DDP in 3 mM NaCl, 1 mM NaH_2PO_4 at pH 6.5, 37 °C. This value is the same as we observe in the presence of excess DNA, and it agrees well with values for the first hydrolysis of *cis*-DDP measured by Bodenner et al.[8] at 37 °C, namely, 11×10^{-5} s^{-1} in 5 mM $NaNO_3$ and 8.7×10^{-5} s^{-1} in 5 mM phosphate, and by Segal and Le Pecq,[40] $11 \pm 5 \times 10^{-5}$ s^{-1}. It is also similar, allowing for differences due to temperature, phosphate concentration, and pH, to the values of 2.5×10^{-5} s^{-1} measured for the first hydrolysis of *cis*-DDP in water at 25 °C[37] and 8×10^{-5} s^{-1} at 37 °C in 100 mM phosphate.[41] In addition, Bodenner et al. observed a rate constant of $6.2–6.9 \times 10^{-5}$ s^{-1} for the initial binding of *cis*-DDP to DNA at 37 °C,[8] which is close to our figure and to the value of $3.3 \pm 0.6 \times 10^{-5}$ s^{-1} reported by Ushay and co-workers.[7]

During the reaction of *cis*-DDP with DNA, we observed no peaks due to formation of either *cis*-$[Pt(NH_3)_2(H_2O)Cl]^+$ (δ = −1841 ppm) or *cis*-$[Pt(NH_3)_2(H_2O)_2]^{2+}$ (δ = −1593 ppm), indicating either that the reaction proceeds via direct nucleophilic attack on the complex by DNA or that the aquated species react with DNA rapidly as they are formed. The latter explanation is most consistent with the observed agreement between the rate constants for disappearance of the complex and for hydrolysis. From the data of Holler et al.,[22] we compute that, under pseudo-first-order reaction conditions, *cis*-$[Pt(NH_3)_2(H_2O)Cl]^+$ binds to DNA with a half-life of 1–2 min. Similarly, the binding of *cis*-$[Pt(NH_3)_2(H_2O)_2]^{2+}$ to DNA is also complete within minutes.[6,8,22] These results indicate that the steady-state concentrations of aquated species formed during the reaction of *cis*-DDP with DNA are very low, explaining why they are not observed in our ^{195}Pt NMR spectra.

In the absence of DNA, hydrolysis of *cis*-DDP in aqueous solutions containing phosphate and chloride ions gives rise to peaks due to *cis*-$[Pt(NH_3)_2(H_2O)Cl]^+$ at −1841 ppm[42,43] and an unknown species at −1736 ppm. This species appears upfield of the region where hydroxide-bridged dimers (δ = −1611, −1516 ppm) and trimers (δ = −1518 ppm) are found.[44] The unidentified complex does not appear when the hydrolysis is carried out in pure water. It may correspond to *cis*-$[Pt(NH_3)_2(OPO_3H)Cl]^-$, an assignment consistent with the 70 to 80 ppm downfield shift expected upon replacing a water ligand with phosphate[42,44] and the known tendency of phosphate to complex reactive platinum species.[8,38]

As *cis*-DDP is consumed, new resonances appear ~150–220 ppm and 300–350 ppm upfield of the *cis*-DDP resonance (Figure 1). The chemical shifts of these resonances are consistent with the presence of mono- and bifunctional adducts (vide infra). The line widths of the ^{195}Pt NMR resonances increase as *cis*-DDP reacts to form first mono- and then bifunctional adducts. This broadening arises from a combination of effects. The first is an increase in nuclear quadrupole relaxation resulting from coordination of two, three, and four ^{14}N nuclei to the platinum center. Second, attachment of platinum to large DNA fragments (M_r = ~26000 Da) increases the rotational correlation time. Last, platinum experiences a variety of local magnetic environments owing to coordination both to different nucleoside bases and to similar bases in different microscopic shielding environments arising from local variations in DNA sequence context.

The total integrated area of the peaks corresponding to bifunctional adducts at the end of the reaction is, on average, 40% less than the area of the peaks due to *cis*- or *trans*-DDP at the start of the reaction. This effect is the result of the non-uniform excitation due to irradiation over a 100-KHz spectral window; peaks at the edge of the window are not irradiated as fully as those in the center. Also, the repetition rate of the data acquisition is faster than the time necessary for platinum nuclei to relax completely. Consequently, peak intensities are a function of both the relaxation time and concentration, making it impossible to compare directly the relative areas of different resonances in terms of the concentrations of the species from which they arise.

The formation and closure of monofunctional adducts follows a time dependence consistent with two successive first-order reactions. The concentration of the intermediate species reaches its maximum at a time $t_{max} = [\ln (k_1/k_2)]/(k_1 - k_2)$. Substituting

(39) Tucker, M. A.; Colvin, C. B.; Martin, D. S. *Inorg. Chem.* **1964**, *3*, 1373.
(40) Aprile, F.; Martin, D. S. *Inorg. Chem.* **1962**, *1*, 551.
(41) Knox, R. J.; Friedlos, F.; Lydall, D. A.; Roberts, J. J. *Cancer Res.* **1986**, *46*, 1972.
(42) Pregosin, P. S. *Ann. Reports NMR Spectrosc.* **1986**, *17*, 285 and references therein.
(43) Appleton, T. G.; Hall, J. R.; Ralph, S. F. *Inorg. Chem.* **1985**, *24*, 4685.
(44) Hollis, L. S. Personal communication.

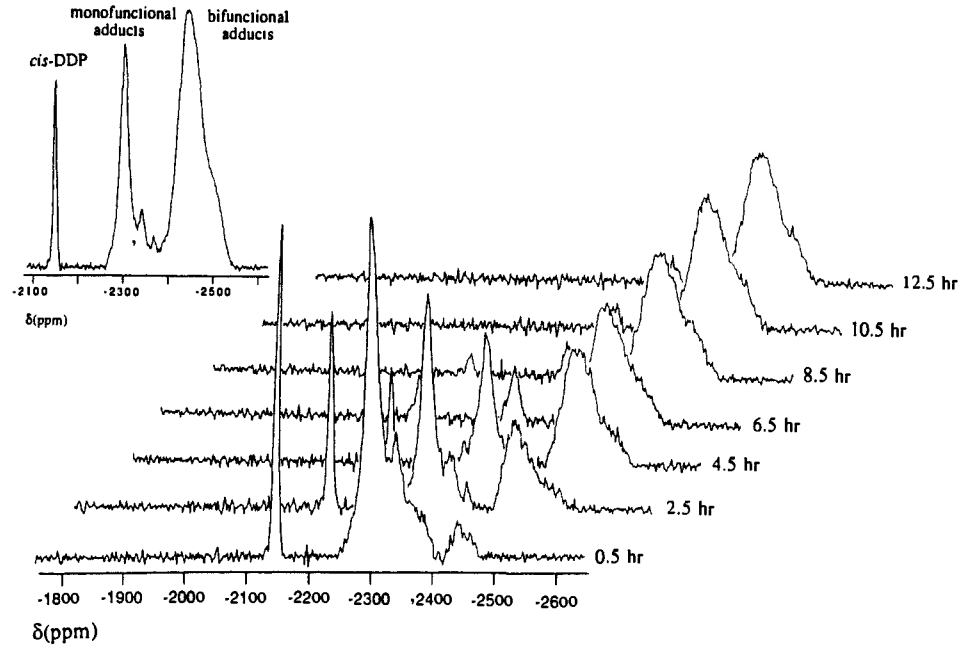

Figure 3. Time course of the reaction between double-stranded chicken erythrocyte DNA and *cis*-$[Pt(NH_3)_2(H_2O)Cl]^+$ at a D/N = 0.07, in 3 mM NaCl and 1 mM NaH_2PO_4, 37 °C, pH 6.5. Each spectrum consists of 200000 transients. The inset shows the sum of the individual spectra.

values of $k_1 = 1 \times 10^{-4}$ s^{-1} for the first hydrolysis of *cis*-DDP (refs 8 and 38 and this work) and $k_2 = 9.3 \times 10^{-5}$ s^{-1} for closure of cis monofunctional adducts (this work) into this expression gives a predicted value for t_{max} of 3 h, consistent with the experimental results.

Reaction of *trans*-DDP with Double-Stranded DNA. The time course of binding of *trans*-DDP to DNA was difficult to observe because it is roughly eight times less soluble than the cis isomer. As shown in Figure 2, *trans*-DDP is consumed in the presence of DNA with a pseudo-first-order rate constant $k = 9.6 \pm 0.4 \times 10^{-5}$ s^{-1}. In the absence of DNA, $k = \sim 9 \times 10^{-5}$ s^{-1}. These rate constants are similar to previously reported values of $k = 9.8 \times 10^{-5}$ [40] and $19 \pm 3 \times 10^{-5}$ s^{-1} [38] for the first hydrolysis of *trans*-DDP in water and to the value of $k = 5.4 \pm 0.9 \times 10^{-5}$ s^{-1} for the binding of *trans*-DDP to DNA.[7]

As noted for the reaction of *cis*-DDP with DNA (vide supra), no aquated species were observed in the corresponding reaction of *trans*-DDP, indicating that such products react rapidly as they are formed. *trans*-$[Pt(NH_3)_2(H_2O)Cl]^+$ reportedly binds to DNA with a second-order rate constant of 0.95 M^{-1} s^{-1} at 25 °C.[6] At the concentration and temperature used here, this rate constant would give a half-life of approximately 20 s, explaining why this species does not accumulate in high enough concentration to be observed by ^{195}Pt NMR spectroscopy. Monofunctional and bifunctional adducts could be observed at chemical shifts similar to those for the cis analogues, but they could not be quantitated accurately due to their low signal-to-noise ratios. Loss of the second chloride ion was clearly established by the presence of bifunctional adducts with ^{195}Pt resonances around −2450 ppm, a result that disagrees with the conclusion of earlier potentiometric determinations.[37]

Reaction of *cis*- and *trans*-$[Pt(NH_3)_2(H_2O)Cl]^+$ with Double-Stranded DNA. Monoaqua analogues of *cis*- and *trans*-DDP were employed to study the kinetics of closure of the cis and trans monofunctional adducts. This reaction can be monitored most accurately in the absence of monofunctional adduct formation. The apparent half-life for closure of *cis*-DDP monofunctional adducts measured from the reaction with *cis*-DDP is roughly 50% longer than that obtained by using the cis monoaqua complex, because monofunctional adducts are being continuously formed during the course of the reaction with the former. Use of the monoaqua complexes is also desirable because their increased solubility allows the reactions to be run at 32 mM rather than 16 mM. This increased concentration, combined with isotopic enrichment of the platinum complexes, affords sufficient signal-to-noise ratios for accurate kinetics measurements to be made with both isomers and also reveals the presence of several minor monofunctional adducts.

The distribution of species obtained by reaction of *cis*-DDP with 1 equiv of $AgNO_3$ in DMF at 0.2 M for 16 h at room temperature has been previously reported.[45,46] In DMF the yield of monosubstituted platinum (O1-DMF, NO_3^-) is higher than that for the corresponding reaction in H_2O. Typically, 80% of the species are monosubstituted and 9% are disubstituted, with only 9–12% of unreacted *cis*-DDP remaining. The present reaction conditions (0.5 M rather than 0.2 M, 37 °C vs room temperature, 1.2 rather than 1.0 equiv of $AgNO_3$) afford less unreacted *cis*-DDP and a slightly higher fraction of disubstituted species. As noted previously, the effect of unreacted *cis*-DDP is to make the observed monofunctional adduct lifetimes appear to be slightly longer than their true values. The presence of disubstituted species does not influence the observed lifetimes of the monofunctional adducts, since they close rapidly to form bifunctional adducts.

Figures 3–6 show the time course of the reactions of *cis*- and *trans*-$[Pt(NH_3)_2(H_2O)Cl]^+$ with double- and single-stranded DNA. At the start of these reactions, the spectra are dominated by large resonances arising from monofunctional adducts and smaller resonances due to *cis*- and *trans*-DDP. The latter complexes arise from incomplete reaction with $AgNO_3$ and, more significantly, back-reaction of monoaquated species with chloride ion in solution. Reaction of monoaquated species with DNA to form monofunctional adducts was usually complete within the few minutes that elapsed between initiation of the reaction and commencement of data collection. Monoaquated species appear in the first spectrum of the *cis*-$[Pt(NH_3)_2(H_2O)Cl]^+$ reactions if data acquisition began within the first 20 min after initiating the reactions. An example appears in Figure 5. The peak at −1840 ppm is assigned to *cis*-$[Pt(NH_3)_2(H_2O)Cl]^+$ and that at −1823 ppm to *cis*-$[Pt(NH_3)_2(DMF)Cl]^+$ or *cis*-$[Pt(NH_3)_2(NO_3)Cl]$, based on previously published chemical shift values for these complexes.[42,43,45,46] Although these species react completely within the first 20 min, it was possible to measure an approximate pseudo-first-order rate constant ($k = 2.0 \pm 0.2 \times 10^{-3}$ s^{-1}, average of two experiments) by using short data acquisition periods (3 min). Since *cis*-$[Pt(NH_3)_2(H_2O)Cl]^+$ reacts much more rapidly

(45) Hollis, L. S.; Amundsen, A. R.; Stern, E. W. *J. Med. Chem.* **1989**, *32*, 128.
(46) Sundquist, W. I.; Ahmed, K. J.; Hollis, L. S.; Lippard, S. J. *Inorg. Chem.* **1987**, *26*, 1524.

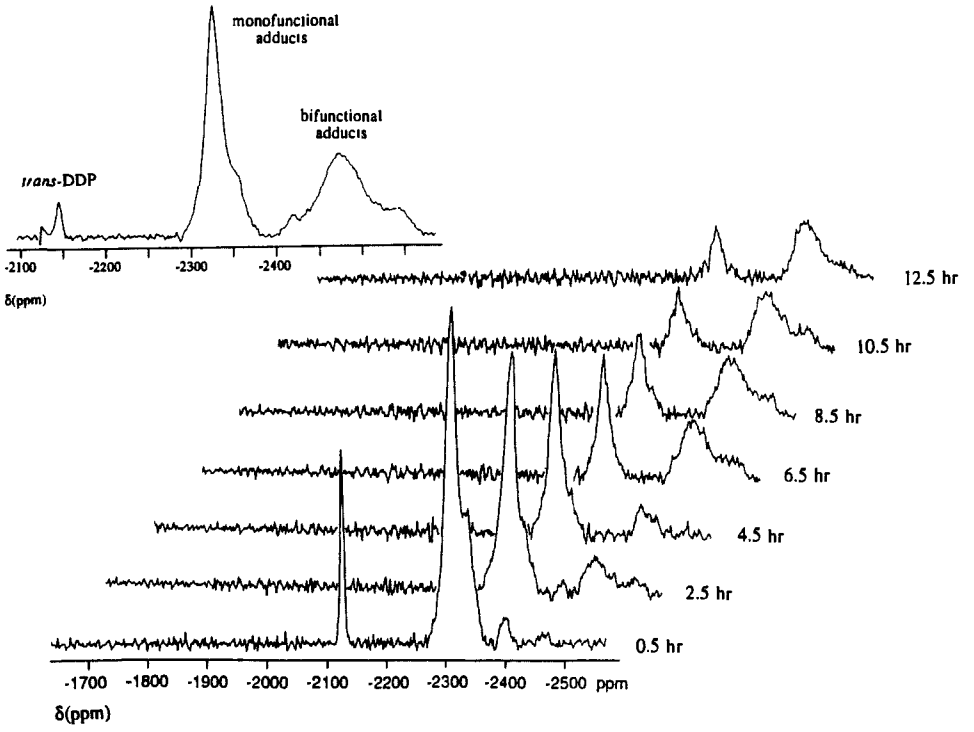

Figure 4. Time course of the reaction between double-stranded chicken erythrocyte DNA and *trans*-$[Pt(NH_3)_2(H_2O)Cl]^+$. The reaction conditions are the same as for Figure 3. The inset shows the sum of the individual spectra.

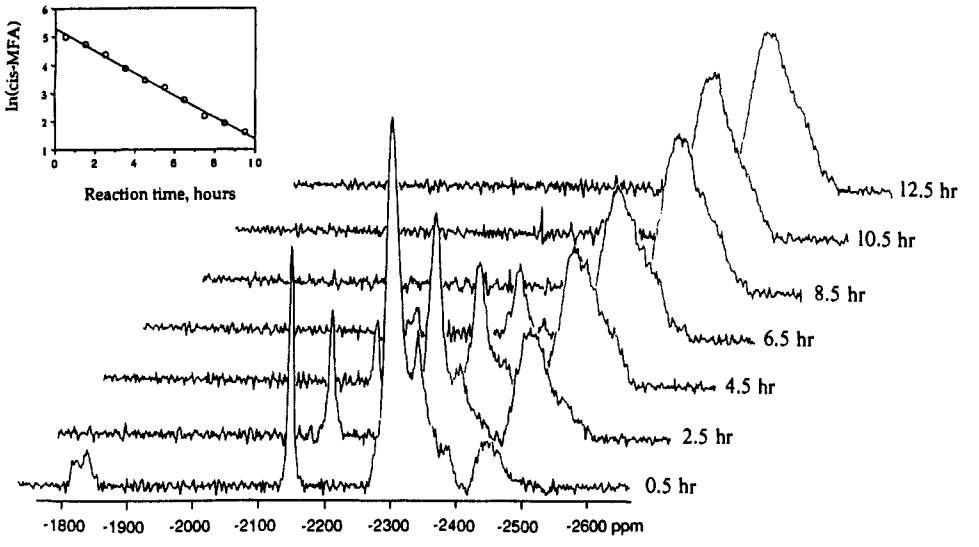

Figure 5. 107.3-MHz ^{195}Pt NMR spectra collected during the course of the reaction between *cis*-$[Pt(NH_3)_2(H_2O)Cl]^+$ and single-stranded chicken erythrocyte DNA. The reaction conditions are as described in Figure 3. The inset shows the plot of ln (*cis*-MFA) vs reaction time, where (*cis*-MFA) is the integrated area of the *cis*-DDP monofunctional adduct resonances.

with DNA (k_2 = 4.3 M^{-1} s^{-1} at 37 °C)[22] than with chloride ion (k_{-1} = 0.015 M^{-1} s^{-1} for $[Pt(en)(H_2O)Cl]^+$),[47] it is expected that most of these species react with DNA rather than reforming *cis*-DDP. Similarly, reformation of *cis*-$[Pt(NH_3)_2(H_2O)Cl]^+$ from *cis*-$[Pt(NH_3)_2(H_2O)_2]^{2+}$ (k_{-1} = 0.31 M^{-1} s^{-1} for $[Pt(en)(H_2O)_2]^{2+}$)[47] competes poorly with direct platination of DNA by *cis*-$[Pt(NH_3)_2(H_2O)_2]^{2+}$ (k_2 = 33.3 M^{-1} s^{-1}).[22] Unreacted monosubstituted species were not observed in the reactions with *trans*-$[Pt(NH_3)_2(H_2O)Cl]^+$.

As shown in the insets of Figures 3 and 4, there are one major and two minor monofunctional adducts formed in the reactions of both *cis*- and *trans*-$[Pt(NH_3)_2(H_2O)Cl]^+$ with DNA. The chemical shifts of these species, listed in Table I, indicate that both isomers form products having similar platinum coordination spheres. By comparing the chemical shifts of resonances arising

(47) Coley, R. F.; Martin, D. S. *Inorg. Chim. Acta* **1973**, *7*, 573.

Table I. ^{195}Pt NMR Peak Assignments for Species Observed in the Reaction of *cis*- and *trans*-DDP with Double-Stranded DNA

species	chemical shift,[a] ppm	assignment
cis-$[Pt(NH_3)_2Cl_2]$	−2149	*cis*-$[Pt(NH_3)_2Cl_2]$
cis monofunctional adducts	−2303 (major)	*cis*-$[Pt(NH_3)_2(N7\text{-}G)Cl]$
	−2342 (minor)	*b*
	−2369 (minor)	*b*
cis bifunctional adducts	−2445 (major)	*cis*-$[Pt(NH_3)_2(N7\text{-}G)_2]$
	−2500 (minor)	*b*
trans-$[Pt(NH_3)_2Cl_2]$	−2145	*trans*-$[Pt(NH_3)_2Cl_2]$
trans monofunctional adducts	−2326 (major)	*trans*-$[Pt(NH_3)_2(N7\text{-}G)Cl]$
	−2354 (minor)	*b*
	−2417 (minor)	*b*
trans bifunctional adducts	−2474 (major)	*trans*-$[Pt(NH_3)_2(N7\text{-}G)_2]$
	−2540 (minor)	*b*

[a] At 37 °C in aqueous solution relative to Na_2PtCl_6 (0 ppm). [b] Not definitively assigned (see text).

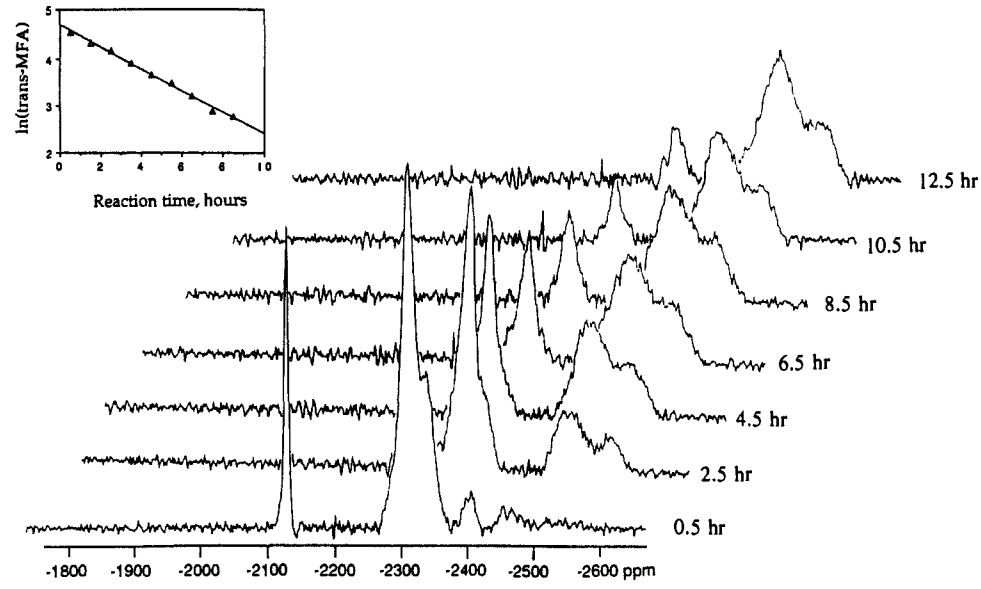

Figure 6. Time course of the reaction between *trans*-$[Pt(NH_3)_2(H_2O)Cl]^+$ and single-stranded chicken erythrocyte DNA. The reaction conditions are as described in Figure 3. The inset shows the plot of ln (*trans*-MFA) vs reaction time, where (*trans*-MFA) is the integrated area of the *trans*-DDP monofunctional adduct resonances.

Table II. ^{195}Pt NMR Chemical Shifts of *cis*- and *trans*-$[Pt(NH_3)_2]^{2+}$ Adducts of Nucleobases: Monofunctional Adduct Models

compound	chemical shift,[a] ppm	ref
cis-$[Pt(NH_3)_2(N7\text{-}dGMP)Cl]^-$	−2302	*b*
cis-$[Pt(NH_3)_2(N7\text{-}dGMP)Cl]^-$	−2295	*c*
cis-$[Pt(NH_3)_2(N7\text{-}dGMP)Cl]^-$	−2297	this work
cis-$[Pt(NH_3)_2(N7\text{-}dG)Cl]^+$	−2280	45
cis-$[Pt(NH_3)_2(N7\text{-}dGMP)(H_2O)]$	−2058	this work
cis-$[Pt(NH_3)_2(N7\text{-}dAMP)Cl]^-$	−2354	*b*
cis-$[Pt(NH_3)_2(N3\text{-}dC)Cl]^+$	−2357	45
cis-$[Pt(NH_3)_2(N3\text{-}dC)Cl]^+$	−2353	43
cis-$[Pt(NH_3)_2(N3\text{-}1\text{-}Me\text{-}Cyt)Cl]^+$	−2365	45
trans-$[Pt(NH_3)_2(N7\text{-}dGMP)Cl]^-$	−2314	this work
trans-$[Pt(NH_3)_2(N7\text{-}dGMP)(H_2O)]$	−2030	this work
trans-$[Pt(NH_3)_2(N1\text{-}pyr)Cl]^+$	−2310	45
$[Pt(NH_3)_3Cl]^+$	−2354	42

[a] Relative to Na_2PtCl_6. [b] Clore, G. M.; Gronenborn, A. M. *J. Am. Chem. Soc.* **1982**, *104*, 1369. [c] Miller, S. K.; Marzilli, L. G. *Inorg. Chem.* **1985**, *24*, 2421.

from the major monofunctional *cis*- and *trans*-DDP adducts with those measured of model complexes (listed in Table II), we assign them as *cis*-$[Pt(NH_3)_2(N7\text{-}pG)Cl]$ and *trans*-$[Pt(NH_3)_2(N7\text{-}pG)Cl]$, respectively. No peaks corresponding to monofunctional adducts having H_2O rather than chloride as the fourth ligand are observed. Such aquated monofunctional adducts would have shifts 240–280 ppm downfield of the monochloro species, as found for *cis*- and *trans*-$[Pt(NH_3)_2(H_2O)(N7\text{-}dGMP)]$ (Table II). The absence of such species suggests that, as reported by other investigators,[22,23] loss of chloride is the rate-determining step for closure as well as formation of the monofunctional adducts. Aquated monofunctional adducts react with a second DNA base seven to eight times faster than the chloro analogues;[22,23] similarly, $[Pt(dien)(H_2O)]^{2+}$ reacts with pyridine 70 times faster than $[Pt(dien)Cl]^+$.[48]

From the chemical shifts of the minor monofunctional adducts it is clear that they also have a $[Pt(NH_3)_2(N)Cl]$ coordination sphere, where N is a nucleobase nitrogen donor. The resonances of these monofunctional adducts appear upfield of those for platinum coordinated to N7 of guanosine and are similar in chemical shift (Table I) to adducts having platinum bonded to N7 of adenosine or N3 of cytosine (Table II).[43,44] The smaller size of these peaks is consistent with the kinetic preference of platinum for GMP > AMP ≫ CMP ≫ UMP.[49]

Monofunctional adducts derived from *cis*- (Figure 3) and *trans*-DDP (Figure 4) are gradually consumed, with concomitant appearance of resonances due to bifunctional adducts. The loss of the *cis*- and *trans*-DDP monofunctional adducts follows pseudo-first-order reaction kinetics (Figure 7), the rate constants for which are given in Table III. Linear least-squares fits to plots of ln (peak area) vs reaction time (Figure 7) give rate constants $k = 9.2 \pm 1.4 \times 10^{-5}$ s^{-1} ($t_{1/2} = 2.1 \pm 0.3$ h, average of four experiments) for the loss of *cis*-DDP monofunctional adducts and $k = 6.3 \pm 0.1 \times 10^{-5}$ s^{-1} ($t_{1/2} = 3.1 \pm 0.1$ h, two experiments) for the *trans*-DDP monofunctional adducts. These results may be compared to values of $k = 8.1 \pm 4 \times 10^{-5}$ s^{-1} obtained for hydrolysis of $[Pt(en)(H_2O)Cl]^+$,[47] $4.2 \pm 0.2 \times 10^{-5}$ s^{-1} measured for the second hydrolysis of *cis*-DDP,[38] 4.5 to 5×10^{-5} s^{-1} seen for closure of cis monofunctional adducts,[23] and 5.5×10^{-5} s^{-1} estimated from the rate of formation of interstrand cross-links.[41] The same rate constants for loss of *cis*- ($k = 9.9 \pm 0.9 \times 10^{-5}$ s^{-1}, two experiments) and *trans*-DDP ($k = 6.3 \times 10^{-5}$ s^{-1}, one experiment) monofunctional adducts were obtained when the reaction was run at lower concentrations of DDP. The rate constants were also independent of pH in the 6.5–7.5 range studied. The correlation between rate constants for monofunctional adduct closure and those for the second hydrolysis of chloride ion in the free complexes is consistent with formation of an aquated intermediate rather than direct displacement of chloride by a second nucleotide on DNA. In the kinetics analysis, the integrals of peaks corresponding to all monofunctional adducts were employed, a treatment that assumes the rate of closure to be independent of adduct type. This assumption is supported by the observation that the rate of *cis*-DDP monofunctional adduct closure is the same on DNA polymers of varying base composition.[23]

One major and one minor bifunctional adduct were observed for both *cis*- and *trans*-DDP, the chemical shifts of which correspond to $Pt(N)_4$ coordination spheres. By comparison with model complexes (Table IV), the major bifunctional adducts are assigned as *cis*- and *trans*-$[Pt(NH_3)_2(N7\text{-}dG)_2]$, consistent with the results of earlier mapping studies.[9-17,21] Bifunctional adducts are stable for days at room temperature in the reaction solution, as monitored by ^{195}Pt NMR spectroscopy, although the ratio of upfield to downfield peak heights increases very slowly with time. This behavior could be analogous to the slow linkage isomerization of a 1,3-*trans*-$[Pt(NH_3)_2\{d(GCG)\}]$ adduct built site-specifically into a dodecamer, which affords 1,4-*trans*-$[Pt(NH_3)_2\{d(CGCG)\}]$

(48) Lim, M. C.; Martin, R. B. *J. Inorg. Nucl. Chem.* **1976**, *38*, 1911.

(49) Mansy, S.; Chu, Y.-H.; Duncan, R. E.; Tobias, R. S. *J. Am. Chem. Soc.* **1978**, *100*, 607.

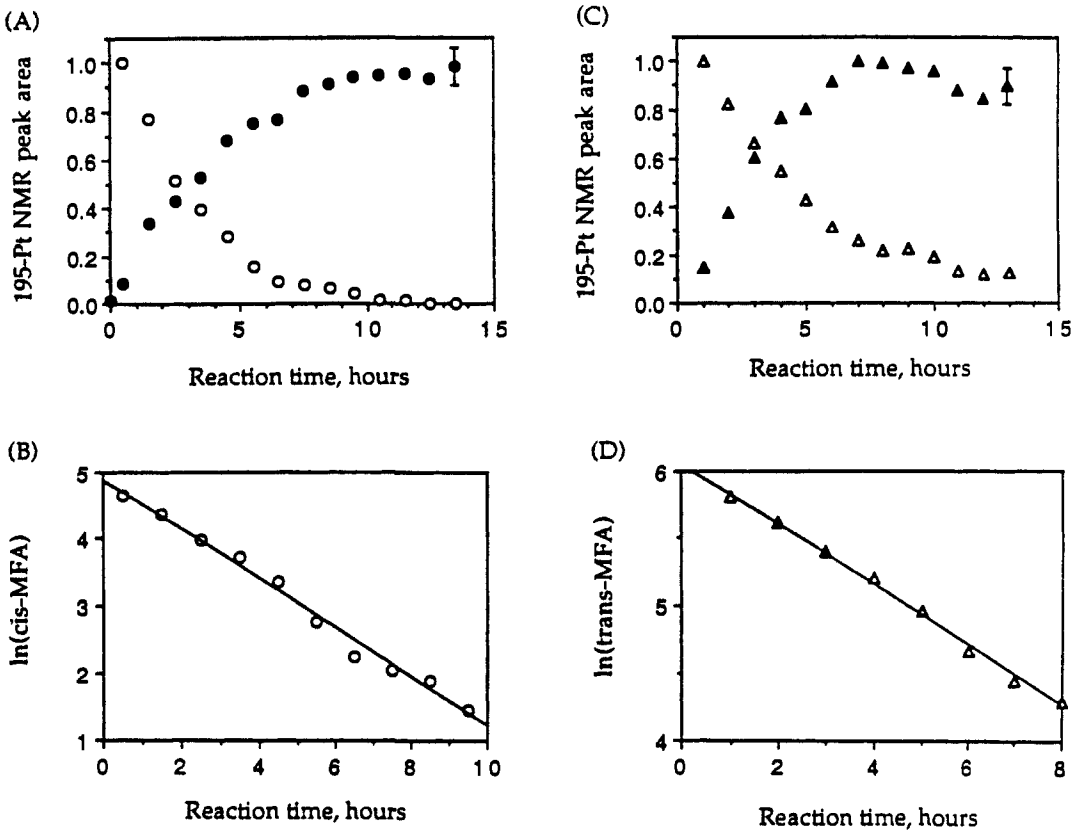

Figure 7. Determination of the rate constants for closure of *cis*- and *trans*-DDP monofunctional adducts. (A) Plots of the normalized ^{195}Pt NMR peak area of the cis monofunctional (open circles) and bifunctional (closed circles) adducts formed during the course of the reaction shown in Figure 3. Bars depicting the average error are shown for one data point. (B) Plot of ln (*cis*-MFA) vs reaction time, where (*cis*-MFA) is the ^{195}Pt NMR peak area of the *cis*-DDP monofunctional adducts. (C) Plots of the normalized ^{195}Pt NMR peak area of the *trans*-DDP monofunctional (open triangles) and bifunctional (closed triangles) adducts formed during the course of the reaction shown in Figure 4. Bars depicting the average error are shown for one data point. (D) Plot of ln (*trans*-MFA) vs reaction time, where (*trans*-MFA) is the ^{195}Pt NMR peak area of the *trans*-DDP monofunctional adducts.

Table III. Rate Constants for the Reactions of *cis*- and *trans*-DDP with DNA in 3 mM NaCl, 37 °C

reaction	product	k, s^{-1}	$t_{1/2}$, h	pH
cis-DDP + (DS) DNA	*cis*-(DS) DNA MFA	$10.2 \pm 0.7 \times 10^{-5}$	1.9 ± 0.1	6.5
cis-DPP + (DS) DNA[b]	*cis*-(DS) DNA MFA	$9.3 \pm 0.2 \times 10^{-5}$	2.1 ± 0.1	7.5
cis-DDP + (SS) DNA	*cis*-(SS) DNA MFA	$10.9 \pm 0.1 \times 10^{-5}$	1.8 ± 0.1	6.5
cis-(DS) DNA MFA	*cis*-(DS) DNA BFA	$9.2 \pm 1.4 \times 10^{-5}$	2.1 ± 0.3	6.5
cis-(DS) DNA MFA	*cis*-(DS) DNA BFA	$8.6 \pm 0.1 \times 10^{-5}$	2.2 ± 0.1	7.3
cis-(SS) DNA MFA	*cis*-(SS) DNA BFA	$10.4 \pm 0.6 \times 10^{-5}$	1.9 ± 0.1	6.5
trans-DDP + (DS) DNA	*trans*-(DS) DNA MFA	$9.6 \pm 0.4 \times 10^{-5}$	2.0 ± 0.1	6.5
trans-(DS) DNA MFA	*trans*-(DS) DNA BFA	$6.3 \pm 0.1 \times 10^{-5}$	3.1 ± 0.1	6.5
trans-(DS) DNA MFA	*trans*-(DS) DNA BFA	$5.5 \pm 0.5 \times 10^{-5}$	3.5 ± 0.3	7.4
trans-(SS) DNA MFA	*trans*-(SS) DNA BFA	$6.8 \pm 0.6 \times 10^{-5}$	2.9 ± 0.3	6.5

[a] Abbreviations: (DS) DNA, double-stranded chicken erythrocyte DNA; (SS) DNA, single-stranded DNA; *cis*-DNA MFA, *cis*-$[Pt(NH_3)_2Cl]$-DNA monofunctional adducts; *trans*-DNA MFA, *trans*-$[Pt(NH_3)_2Cl]$-DNA monofunctional adducts; *cis*-DNA BFA, *cis*-$[Pt(NH_3)_2]$-DNA bifunctional adducts; *trans*-DNA BFA, *trans*-$[Pt(NH_3)_2]$-DNA bifunctional adducts. [b] Sample prepared without heating above 37 °C (see text).

having a ^{195}Pt NMR shift of −2520 ppm.[50]

The rate of bifunctional adduct formation begins to diminish after about 6 h. The resonances were difficult to integrate owing to random noise, broad line widths, and baseline roll. By using peak heights, however, pseudo-first-order rate constants for bifunctional adduct formation were estimated to be within 40% of the values obtained by measuring the loss of the monofunctional adducts.

Reaction of *cis*- and *trans*-$[Pt(NH_3)_2(H_2O)Cl]^+$ with Single-Stranded DNA. As seen in Figures 5 and 6, monoaquated species react with single-stranded DNA to afford a similar distribution of adducts to that observed with double-stranded DNA. This similarity is expected since the preferred platinum binding sites (purine N7) are accessible in both single- and double-stranded forms.

The kinetics of closure of mono-to bifunctional adducts for both isomers on single-stranded DNA are also the same as measured with double-stranded DNA. The pseudo-first-order rate constants, derived from linear least-squares fits to the plots of ln (peak area) vs reaction time (Figures 5 and 6), are listed in Table III. These results differ markedly from literature values obtained by using thiourea to trap the closure of *trans*-DDP monofunctional adducts.[16] From this approach it was reported that closure of *trans*-DDP monofunctional adducts on double-stranded DNA is much slower than on single-stranded DNA, with a half-life of roughly 24 h. The present ^{195}Pt NMR experiments show that the closure of *trans*-DDP monofunctional adducts on double-stranded DNA (Figure 3) is nearly complete after 12 h and that the rate constant is an order of magnitude larger than estimated, by assuming first-order kinetics, from the literature result.[16]

Determination of Activation Parameters. In order to provide further mechanistic insight into the reaction, approximate values for the enthalpy ($\Delta H^{\ddagger}$) and entropy ($\Delta S^{\ddagger}$) of activation for closure

(50) Comess, K. M.; Costello, C. E.; Lippard, S. J. *Biochemistry* **1990**, *29*, 2102.

Table IV. ^{195}Pt NMR Chemical Shifts of *cis*- and *trans*-$[Pt(NH_3)_2]$-Nucleic Acid Complexes; Bifunctional Adduct Models

compound	chemical shift[a]	ref
cis-$[Pt(NH_3)_2(N7\text{-}dGMP)_2]^{2-}$	-2451	*b*
cis-$[Pt(NH_3)_2(N7\text{-}dGMP)_2]^{2-}$	-2455	*c*
cis-$[Pt(NH_3)_2(N7\text{-}dGMP)_2]^{2-}$	-2434	this work
cis-$[Pt(NH_3)_2\{d(GpTpG)\text{-}N7,N7\}]$	-2460	this work
cis-$[Pt(NH_3)_2\{d(ApG)\text{-}N7,N7\}]^{+}$	-2462	this work
cis-$[Pt(NH_3)_2(N7\text{-}AMP)_2]^{2-}$	-2479	*d*
$[Pt(en)(N7\text{-}dAMP)_2]^{2-}$	-2685, -2690	*d*
trans-$[Pt(NH_3)_2(N7\text{-}dGMP)_2]^{2-}$	-2469	this work
trans-$[Pt(NH_3)_2\{d(GpCpG)\text{-}N7,N7\}]$	-2470	this work
trans-$[Pt(NH_3)_2\{d(TCTACGCGTTCT)$-G6-N7,G8-N7$\}]$	-2437	50
trans$[Pt(NH_3)_2\{d(TCTACGCGTTCT)$-C5-N3,G8-N7$\}]$	-2520	50

[a] Relative to Na_2PtCl_6. [b] Clore, G. M.; Gronenborn, A. M. *J. Am. Chem. Soc.* **1982**, *104*, 1369. [c] Miller, S. K.; Marzilli, L. G. *Inorg. Chem.* **1985**, *24*, 2421. [d] Reily, M. D.; Marzilli, L. G. *J. Am. Chem. Soc.* **1986**, *108*, 6785.

of *cis*- and *trans*-DDP monofunctional adducts were determined from the temperature dependence of the rates of closure. Rate constants and activation parameters, calculated from a linear least-squares fit to plots of ln (k/T) vs $1/T$ (Figure 8),[51] are reported in Table V. The derived values are imprecise owing to the narrow accessible temperature range (30–45 °C). Temperatures below 30 °C could not be studied because of solubility limitations and increased solution viscosity; marked broadening of the resonances occurred even at 30 °C. Temperatures above 45 °C were not employed, both in order to avoid DNA melting and because data could not be collected rapidly enough to determine accurate rate constants at the higher reaction rates. Interestingly, the mono- and bifunctional adduct resonances are considerably narrower at elevated temperatures, implying that the line broadening is predominantly a function of the rotational correlation time. It is important to note that, since calculated activation parameters are based upon the closure rates of a family of monofunctional adducts rather than a single species, the values obtained best reflect closure of the most abundant species, *cis*- and *trans*-$[Pt(NH_3)_2(N7\text{-}dG)Cl]$.

The low enthalpies and negative entropies of activation are consistent with an associative transition state[52,53] and are in reasonably good agreement with values measured for other substitution reactions of square-planar Pt(II) complexes, listed in Table VI. In particular, the activation parameters for the reaction of *cis*-DDP with DNA are, within experimental error, the same as those measured for the substitution of the first chloride of *cis*-DDP by H_2O.[39]

Although negative activation entropies are consistent with an associative mechanism, they alone do not distinguish between a reaction pathway involving association of solvent versus direct nucleophilic attack by a donor atom on DNA. Such a distinction can be made by measuring the chloride ion dependence of the pseudo-first-order rate constant; a solvolysis mechanism would be chloride dependent, whereas an S_N2 type mechanism would not. Although the effect of chloride ions upon the rate constants could not be studied in our system, owing to DNA aggregation at higher salt concentrations, others have previously reported the existence of such a dependence for the closure of *cis*-DDP monofunctional adducts.[22,23] Thus, both initial binding of *cis*-DDP and subsequent closure of monofunctional adducts most likely proceeds via solvent-assisted pathways, as observed for many square-planar substitution reactions.[52,53] We cannot completely eliminate the possibility of direct displacement of chloride by a neighboring base, however, which could account for the more negative $\Delta S^{\ddagger}$ value observed for closure of the monofunctional *trans*-DDP adducts. Although not specifically addressed in the present study, the *cis*-DDP bifunctional adducts are primarily 1,2-intrastrand cross-links whereas those formed by *trans*-DDP are most likely 1,3- and longer range-intrastrand cross-links.[9-19] Formation of the latter would require a more organized transition state in a nonsolvolytic pathway.

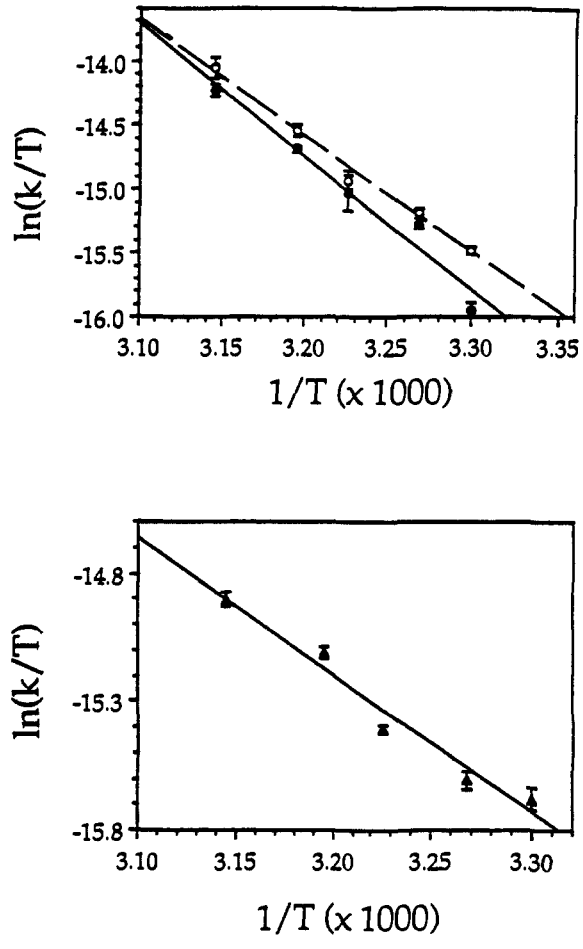

Figure 8. Plot of ln (k/T) vs $1/T$ for the reaction of *cis*-DDP and *trans*-DDP with double-stranded DNA in 3 mM NaCl, pH 6.5. Top: results for the initial reaction of *cis*-DDP with DNA (dashed line) and the closure of *cis*-DDP monofunctional adducts (solid line). Bottom: results for the closure of *trans*-DDP monofunctional adducts.

Effect of Glutathione upon the Closure of *cis*- and *trans*-DDP Monofunctional Adducts. Loss of *cis*-DDP monofunctional adducts in the presence of 5 mM glutathione (0.16 equiv per mol of Pt) proceeds with a slightly shorter half-life (1.6 h) than in its absence. Bifunctional adducts form in the usual way. When the same reaction is carried out in the presence of 23 mM glutathione (0.7 equiv per mol of Pt), however, *cis*-DDP monofunctional adducts are completely consumed within 3 h, considerably faster than in the absence of this sulfhydryl agent (vide supra). As shown in Figure 9, apart from bifunctional DNA adducts, two additional products appear having ^{195}Pt NMR chemical shifts of -2898 and -2913 ppm. Comparison of these values with those of model complexes indicates the new products to have a PtN_3S coordination sphere (-2800 to -3200 ppm). Compositions such as $PtN_2(O)(S)$ (-2700 to -2800 ppm) or PtN_2S_2 (-3200 to -3600 ppm) can be ruled out on the basis of their different chemical shifts.[42,43,54,55] The solutions slowly developed a yellow color, consistent with formation of a previously reported polymeric species ($M_r > 30000$)

(51) Eyring, H. *Chem. Rev.* **1935**, *17*, 65.
(52) Basolo, F.; Pearson, R. G. *Mechanisms of Inorganic Reactions*, 2nd ed.; John Wiley and Sons: New York, 1967; p 405.
(53) Langford, C. H.; Gray, H. B. *Ligand Substitution Processes*; W. A. Benjamin: London, 1966; p 43.
(54) Appleton, T. G.; Conner, J. W.; Hall, J. R. *Inorg. Chem.* **1988**, *27*, 130.
(55) Lempers, E. L.; Inagaki, K.; Reedijk, J. *Inorg. Chim. Acta* **1988**, *152*, 201.

Table V. Rate Constants ($\times 10^5$) and Activation Parameters for Reactions of *cis*- and *trans*-DDP with Double-Stranded DNA

reaction	product	k, s^{-1} 30 °C	33 °C	37 °C	40 °C	45 °C
cis-DDP + DNA	*cis*-DNA MFA	5.7 ± 0.2	7.8 ± 0.2	10.2 ± 0.7	15.1 ± 0.8	25 ± 2
cis-DNA MFA	*cis*-DNA BFA	3.6 ± 0.2	7.1 ± 0.3	9.2 ± 1.4	13.1 ± 0.3	21 ± 1
trans-DNA MFA	*trans*-DNA BFA	4.7 ± 0.2	5.1 ± 0.2	6.3 ± 0.1	8.5 ± 0.2	10.7 ± 0.3

reaction	product	ΔH^*, kcal/mol	ΔS^*, eu
cis-DDP + DNA	*cis*-DNA MFA	18 ± 1	−18 ± 3
cis-DNA MFA	*cis*-DNA BFA	21 ± 2	−10 ± 7
trans-DNA MFA	*trans*-DNA BFA	11 ± 1	−44 ± 3

[a] Abbreviations: *cis*-DNA MFA, *cis*-{$Pt(NH_3)_2Cl$}-DNA monofunctional adducts; *trans*-DNA MFA, *trans*-{$Pt(NH_3)_2Cl$}-DNA monofunctional adducts, *cis*-DNA BFA, *cis*-{$Pt(NH_3)_2$}-DNA bifunctional adducts; *trans*-DNA BFA, *trans*-{$Pt(NH_3)_2$}-DNA bifunctional adducts.

Table VI. Activation Parameters for the Substitution Reactions of Pt(II) in Aqueous Solution[a]

complex	entering group	ΔH^*, kcal/mol	ΔS^*, eu	ref
cis-$[Pt(NH_3)_2Cl_2]$	H_2O	19	−15	39
cis-$[Pt(NH_3)_2Cl_2]$	DMSO	20	−12	46
$[Pt(en)Cl_2]$	H_2O	20	−10	47
$[Pt(en)(H_2O)Cl]^+$	H_2O	8	−50	47
trans-$[Pt(NH_3)_2Cl_2]$	H_2O	20	−11	39
trans-$[Pt(NH_3)_2Cl_2]$	DMSO	17	−1	46
$[Pt(NH_3)_3Cl]^+$	H_2O	18	−18	47

[a] Adapted from ref 53.

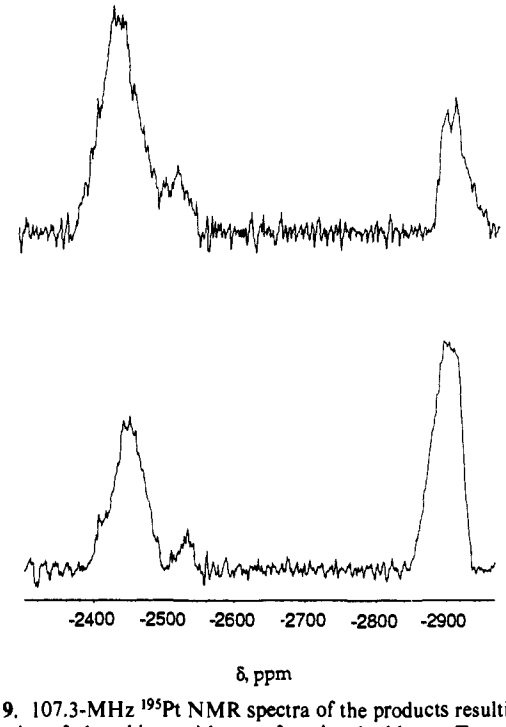

Figure 9. 107.3-MHz ^{195}Pt NMR spectra of the products resulting from the reaction of glutathione with monofunctional adducts. Top: reaction of *cis*-DDP monofunctional adducts on double-stranded DNA for 16 h with 0.7 equiv (23 mM) of reduced glutathione. Bottom: reaction of *trans*-DDP monofunctional adducts for 16 h with 0.7 equiv (23 mM) of reduced glutathione.

having two glutathione ligands bound per platinum atom,[26] that was not observed by ^{195}Pt NMR spectroscopy.[56]

The closure of *trans*-DDP monofunctional adducts in the presence of 5 mM glutathione occurs with a half-life of 2.6 h and forms, in addition to bifunctional adducts, one new major and one minor product with resonances at −2906 and −2940 ppm, respectively. Continued reaction at room temperature for 21 h resulted in no further spectral change, indicating that the glutathione trapped products were relatively stable. Subsequent precipitation of the DNA with one volume of 2-propanol revealed

(56) Abbott, E. H.; Lippard, S. J. Unpublished results.

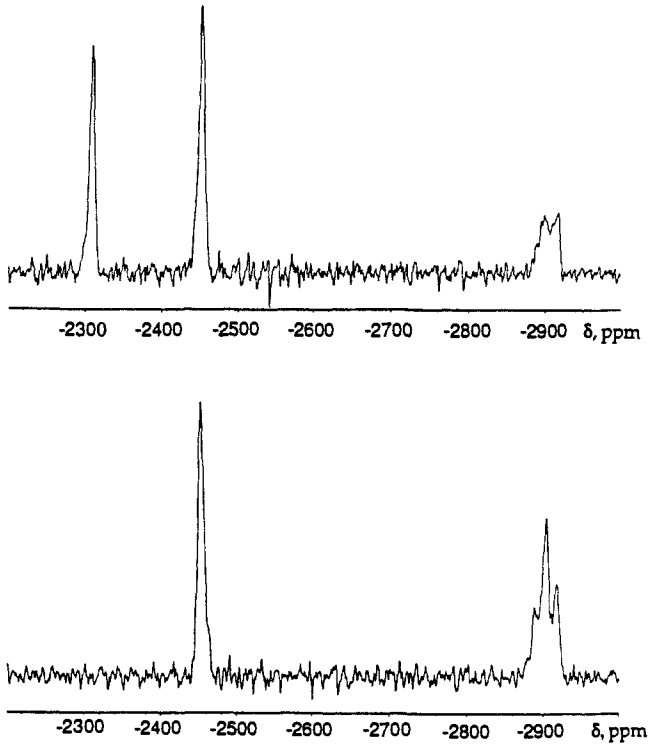

Figure 10. 107.3-MHz ^{195}Pt NMR spectral study of the reaction of a mixture of *trans*-$[Pt(NH_3)_2(dGMP)Cl]^-$ and *trans*-$[Pt(NH_3)_2(dGMP)_2]^{2-}$ with 1 equiv (10 mM) of glutathione in 3 mM NaCl and 1 mM NaH_2PO_4, at 37 °C. Top: beginning of reaction (0 to 1 h). Bottom: end of reaction (after 16 h).

that the new product precipitated with the nucleic acid. It therefore must either be bound to DNA or a water soluble polymer. The supernatant contained no platinum species having ^{195}Pt resonances in the −2100 to −3600 ppm range.

The reaction of a mixture of *trans*-$[Pt(NH_3)_2(dGMP)Cl]^-$ and *trans*-$[Pt(NH_3)_2(dGMP)_2]^{2-}$ with 1 equiv of glutathione for 16 h at 37 °C gave a pattern of NMR resonances similar to that observed for the reaction of glutathione with *trans*-DDP monofunctional adducts (Figure 10). The *trans*-$[Pt(NH_3)_2(dGMP)Cl]^-$ resonance disappeared completely over the reaction time course, while that due to *trans*-$[Pt(NH_3)_2(dGMP)_2]^{2-}$ was unaffected. The products of glutathione with *trans*-$[Pt(NH_3)_2(dGMP)Cl]^-$ have resonances with chemical shifts of −2903, −2888, and −2917 ppm. Since formation of high molecular weight, polymeric platinum–glutathione species is unlikely at a ratio of only one glutathione per five platinum atoms, the major product (δ −2900 ppm) is most likely a trapped monofunctional adduct of the type *trans*-$[Pt(NH_3)_2(N7\text{-}pGp)(S\text{-}glutathione)]$.

In the presence of 23 mM glutathione (0.7 equiv per mol of Pt), the *trans*-DDP monofunctional adducts disappeared by the end of the first hour, consistent with a direct, second-order reaction with the glutathione. As seen in Figure 9, in addition to peaks arising from bifunctional adducts, a large resonance appeared at −2900 ppm, in the region expected for glutathione-containing species. Incubation of *cis*- and *trans*-DDP bifunctional adducts

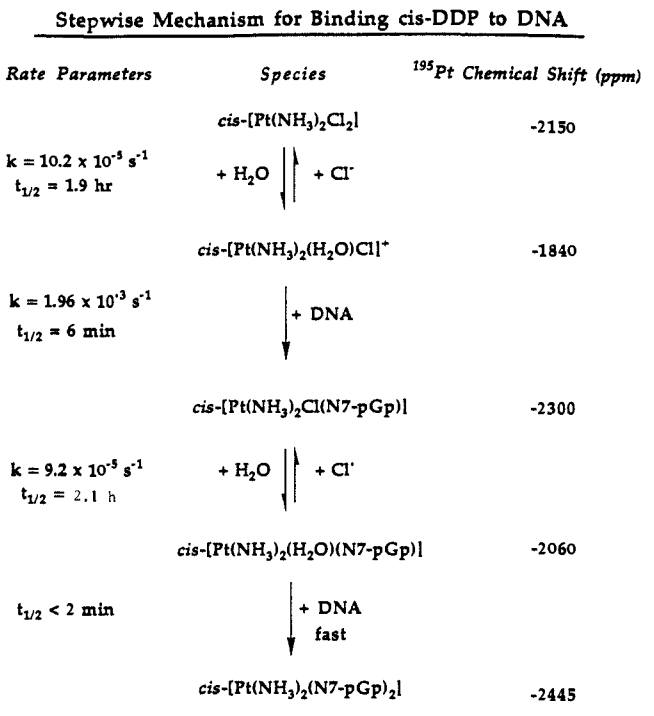

Figure 11. Proposed mechanism for the binding of *cis*-DDP to double-stranded DNA.

with 5 mM glutathione (0.16 equiv) for 24 h at 37 °C, followed by incubation with 25 mM glutathione (0.8 equiv) for an additional 24 h, gave no apparent formation of glutathione-bound platinum species.

The present results for the reaction of glutathione with monofunctional adducts are consistent with earlier work[13,14] reporting that *trans*-DDP monofunctional adducts are more reactive toward glutathione than those of *cis*-DDP, while bifunctional adducts of both isomers are unreactive. The preference of monofunctional adducts to bind glutathione rather than a second DNA base was previously suggested by the observation that the monofunctional adduct analogue $[Pt(dien)Cl]^+$ binds exclusively to glutathione in the presence of a 10-fold excess of 5′-GMP.[55]

Conclusions and Biological Relevance

We propose the following mechanism, summarized in Figure 11, for the stepwise binding of *cis*- and *trans*-DDP to DNA. The rate-determining step for initial binding is hydrolysis of the first chloride ion via association of solvent water ($t_{1/2}$ 1.9 h). The monoaquated species rapidly bind DNA, predominantly at the N7 position of guanosine, to form monofunctional adducts. We speculate that, in vivo, the positive charge of the $[Pt(NH_3)_2(H_2O)Cl]^+$ ion facilitates its diffusion to DNA, a polyanion, followed by rapid diffusion along the double helix to the most favorable binding sites, the very nucleophilic purine N7 positions. The rate-determining step for closure of the monofunctional adducts is hydrolysis of the second chloride ion, again by a solvent-assisted mechanism ($t_{1/2}$ = 2.1 h for *cis*-DDP and 3.1 h for *trans*-DDP at pH 6.5). The aquated monofunctional adducts react rapidly with the endocyclic nitrogen atom of a second base to form bifunctional adducts.

The similarity in half-lives for monofunctional adducts of *cis*- and *trans*-DDP on DNA clearly demonstrates that, contrary to the suggestion of other investigators,[14,17] the biological inactivity of *trans*-DDP is not due to an inherently slower rate of closure for the monofunctional adducts. Furthermore, the kinetics of initial binding of *cis*-DDP and closure of both isomers using single-stranded DNA are the same as for duplex DNA.

Glutathione rapidly binds *trans*-DDP monofunctional adducts to form products having ^{195}Pt chemical shifts indicative of PtN_3S coordination. We assign this spectral feature to a sulfur-bound, glutathione-trapped monofunctional adduct. *cis*-DDP monofunctional adducts react less avidly with glutathione, but at higher glutathione concentrations they form products with similar chemical shifts. Glutathione does not appear to react with *cis*- or *trans*-DDP bifunctional adducts. These results are consistent with previous work suggesting that the biological inactivity of *trans*-DDP may be the result of selective trapping of monofunctional adducts before they close to form bifunctional lesions,[13,14] which are known to inhibit DNA synthesis as effectively as those of the *cis*-DDP analogue.[5,21] Our data reveal, however, that the greater propensity of glutathione to bind to *trans*-DDP monofunctional adducts is due to their faster rate of binding to the sulfur-containing nucleophile rather than to differences in the half-lives of the monofunctional adducts of *cis*- and *trans*-DDP.

In addition to trapping monofunctional adducts, binding of glutathione to free *trans*-DDP may generate DNA–Pt–glutathione cross-linked species by a second mechanism. Once bound to a labile site, glutathione will tend to labilize the trans chloride ion, facilitating platinum coordination to DNA. Support for this model may be found in the observation that *trans*-$[Pt(NH_3)_2(DMSO)Cl]Cl$ binds to DNA two to three times more rapidly than *trans*-DDP.[46] In the presence of excess glutathione, however, platinum will most likely bind preferentially to a second thiol rather than DNA.

The possibility that glutathione may intercept *trans*-DDP and its monofunctional DNA adducts before bifunctional adducts can be formed is consistent with the observation that depletion of glutathione increases the sensitivity of ovarian carcinoma cells to *trans*- but not to *cis*-DDP.[57] Once trapped by glutathione, monofunctional adducts of both isomers may be repaired by cellular processes or may be rendered ineffective at disrupting reactions that require a DNA template. Since the spectrum of adducts formed by *trans*-DDP in vivo is not yet available, it remains to be seen whether *trans*-DDP bifunctional adducts form in significant quantities under physiological conditions.

In assessing the biological relevance of this work it is important to note that, although very high DNA concentrations were required for these kinetic studies, the rates of monofunctional adduct closure are independent of the DNA concentration as long as pseudo-first-order conditions obtain ($(D/N)_b < 0.1$). Thus, it is likely that the mechanistic conclusions apply to DNA and platinum concentrations found in vivo. Furthermore, the results obtained are consistent with the idea, and support the postulate, that loss of chloride is the rate-determining step in both the initial binding of *cis*- and *trans*-DDP to DNA and the closure of their monofunctional adducts. Finally, the monofunctional adduct closure rates observed here differ from the results of several studies where chemical reagents were used to trap them. In some cases, the discrepancy between the various results is not immediately obvious from the experimental protocols. Preliminary ^{195}Pt NMR kinetic studies of the reactions of platinum complexes with ammonium bicarbonate, a trapping reagent used to quench monofunctional adducts, indicate one source of error to be the assumption that complete inactivation occurs on a time scale fast enough for investigating Pt–DNA binding reactions.

Finally, the results reported herein demonstrate that ^{195}Pt NMR spectroscopy can be applied successfully to the study of platinum–DNA interactions, despite an earlier prediction that, "there is little hope of being able to use such methods to study the compound (*cis*-DDP) bound to native DNA."[58] Additional applications of this powerful methodology should soon be forthcoming.

Acknowledgment. This work was supported by U.S. Public Health Service Grant CA34992 from the National Cancer Institute. D.P.B. is grateful to the National Institute of General Medical Sciences for a National Research Service Award (GM 11880). The ^{195}Pt NMR experiments were performed with the assistance of J. Simms and the staff of the M.I.T. Chemistry Department Spectrometry Laboratory. We thank Drs. J. Norton and J. Bentsen for assistance in analyzing the kinetics results, Drs. E. Abbott and S. Hollis for useful discussions regarding platinum

(57) Richon, V. M.; Schulte, N.; Eastman, A. *Cancer Res.* **1987**, *47*, 2056.
(58) Santos, R. A.; Chien, W.-J.; Harbison, G. S.; McCurry, J. D.; Roberts, J. E. *J. Magn. Reson.* **1989**, *84*, 357.

NMR parameters and chemical shifts, and Dr. J. Hoeschle for assistance in procuring isotopically enriched ^{195}Pt.

Registry No. *cis*-DDP, 15663-27-1; *trans*-DDP, 14913-33-8; *cis*-$[Pt(NH_3)_2(H_2O)Cl]^+$, 53861-42-0; *cis*-$[Pt(NH_3)_2(DMF)Cl]^+$, 79084-70-1; *trans*-$[Pt(NH_3)_2(DMF)Cl]^+$, 128707-47-1; *trans*-$[Pt(NH_3)_2(H_2O)Cl]^+$, 44046-05-1; *trans*-$[Pt(NH_3)_2(dGMP)Cl]^-$, 128660-88-8; *trans*-$[Pt(NH_3)_2NdGMP)_2]^{2+}$, 128683-54-5; *cis*-$[Pt(NH_3)_2(N7\text{-}dGMP)Cl]^-$, 128707-48-2; *cis*-$[Pt(NH_3)_2(N7\text{-}dGMP)(H_2O)]$, 76243-63-5; *trans*-$[Pt(NH_3)_2(N7\text{-}dGMP)(H_2O)]$, 76250-59-4; *cis*-$[Pt(NH_3)_2(N7\text{-}dGMP)_2]^{2-}$, 111348-17-5; *cis*-$[Pt(NH_3)_2\{d(GpTpG)\text{-}N7,N7\}]$, 128660-89-9; *cis*-$[Pt(NH_3)_2\{d(ApG)\text{-}N7,N7\}]^+$, 128660-90-2; *trans*-$[Pt(NH_3)_2\{d(GpcpG)\text{-}N7,N7\}]$, 128683-55-6; deoxyguanosine, 961-07-9; glutathione, 70-18-8.

Pressure Effects on Bimolecular Reductive Quenching of the Platinum(II) Dimer $Pt_2(\mu\text{-}\eta^2\text{-}H_2P_2O_5)_4^{4-}$ by Organic Substrates

Daniel R. Crane and Peter C. Ford*

Contribution from the Department of Chemistry and the Quantum Institute, University of California, Santa Barbara, California 93106. *Received February 26, 1990*

Abstract: Pressure effects are reported for the quenching dynamics of the lowest energy excited state of the d^8-d^8 dimer $Pt_2(\mu\text{-}\eta^2\text{-}H_2P_2O_5)_4^{4-}$ ($^3Pt_2$*). Volumes of activation (ΔV^*) are reported for the H atom abstraction by $^3Pt_2$* from various organic substrates and for O_2 quenching of $^3Pt_2$* in methanol solution. The H atom donors studied include a series of benzyl alcohols, allyl alcohol, tributyltin hydride, and benzyl methyl ether. Volumes of activation of -5.4 ± 0.6 cm^3 mol^{-1} and -4.1 ± 0.7 cm^3 mol^{-1} have been measured for quenching by benzyl alcohol and benzyl methyl ether, respectively. These negative ΔV^* values suggest an associative interaction between the excited state dimer and the H atom donor. The mechanistic implications of the pressure effects on the rates for other quenchers are discussed.

Introduction

The d^8-d^8 dimer of platinum(II) $Pt_2(\mu\text{-}\eta^2\text{-}H_2P_2O_5)_4^{4-}$ (subsequently denoted as $Pt_2(POP)_4^{4-}$ or Pt_2) has drawn considerable attention with regard to its photochemical and photophysical properties in solution.[1] This remarkable metal complex displays

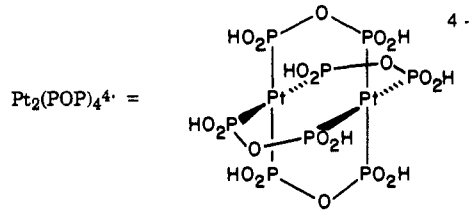

weak fluorescence and strong, long-lived phosphorescence in its ambient temperature luminescence spectrum, with a lifetime of about 10 μs and a quantum yield of 0.55 mol/einstein in aqueous solution.[2] Furthermore, the long-lived triplet excited-state $^3Pt_2$* has been shown to be active in two-electron processes of interest with respect to the conversion of photochemical radiant energy to chemical potential energy.[3] An example is the photodehydrogenation of alcohols to the homologous ketone for which a sequence of steps such as described in Scheme I might be proposed. The monohydride and dihydride species, Pt_2H and Pt_2H_2, have been demonstrated[4] to form under conditions relevant to the photodehydrogenation; Pt_2H_2 has been shown to undergo H_2 when photolyzed,[4b] but the manner by which Pt_2H_2 forms is uncertain.[4c] Participation in similar photocatalytic cycles leads

Scheme I

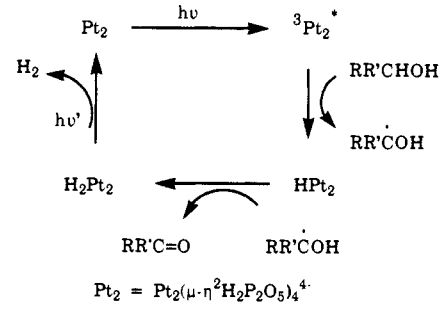

to quenching of the $^3Pt_2$* phosphorescence by a number of different substrates including halogenated hydrocarbons,[5,6] main group hydrides,[5a] and various alcohols.[4a] Although atom abstraction to give an organic free radical plus a Pt(II)-Pt(III) mixed valence dimer is considered to be the probable first step of photoredox paths such as that illustrated by Scheme I, the mechanisms of these chemical quenching pathways are not well characterized.

A technique that has provided valuable mechanistic insight into the intimate mechanisms of both thermal and photochemical reactions is the investigation of pressure effects on reaction dynamics.[7,8] Although there have been several studies on the effect of pressure on the unimolecular deactivation pathways of metal complex excited states,[9] little work has been reported for pressure

(1) (a) Roundhill, D. M.; Gray, H. B.; Che, C.-M. *Acc. Chem. Res.* **1989**, *22*, 55-61, (b) Zipp, A. P. *Coord. Chem. Rev.* **1988**, *84*, 47-83.
(2) Peterson, J. R.; Kalyanasundaram, K. *J. Phys. Chem.* **1985**, *89*, 2486-2492.
(3) Roundhill, D. M. *J. Am. Chem. Soc.* **1985**, *107*, 4354-4356.
(4) (a) Roundhill, D. M.; Atherton, S. J.; Shen, Z.-P. *J. Am. Chem. Soc.* **1987**, *109*, 6076-6079. (b) Harvey, E. L.; Stiegman, A. E.; Vlcek, A.; Gray, H. B. *J. Am. Chem. Soc.* **1987**, *109*, 5233-5235. (c) Harvey, P. D.; Gray, H. B. *New. J. Chem.* **1987**, *11*, 595-596.
(5) (a) Vlcek, A., Jr.; Gray, H. B. *J. Am. Chem. Soc.* **1987**, *109*, 286-287. (b) Marshall, J. L.; Stiegman, A. E.; Gray, H. B. In *Excited States and Reactive Intermediates*; Lever, A. B. P., Ed.; ACS Symposium Series Vol. 307; American Chemical Society: Washington, DC, 1986; pp 166-176.
(6) Roundhill, D. M.; Shen, Z.-P.; King, C.; Atherton, S. J. *J. Phys. Chem.* **1988**, *92*, 4088-4094.
(7) (a) van Eldik, R.; Asano, T.; le Noble, W. J. *Chem. Rev.* **1989**, *89*, 549-688. (b) *Inorganic High Pressure Chemistry: Kinetics and Mechanism*; van Eldik, R., Ed.; Elsevier: New York, 1987.
(8) (a) DiBenedetto, J.; Ford, P. C. *Coord. Chem. Rev.* **1985**, *64*, 361-382. (b) Ford, P. C., Chapter 6 in ref 7b, pp 295-338.

0002-7863/90/1512-6871$02.50/0